Human breast adipose-derived stem cells: Characterization and differentiation into mammary gland-like epithelial cells promoted by autologous activated platelet-rich plasma

SHI-EN CUI[1*], HONG-MIAN LI[2*], DA-LIE LIU[3], HUA NAN[3], KUN-MING XU[2], PEI-RAN ZHAO[4] and SHUANG-WU LIANG[4]

[1]Department of Mammary Gland Surgery, Zhongshan Hospital of Sun Yat-Sen University, Zhongshan, Guangdong 528403; [2]Department of Plastic and Aesthetic Surgery, Zhongshan Bo'ai Hospital of Southern Medical University, Zhongshan, Guangdong 528403; [3]Department of Plastic and Reconstructive Surgery, Zhujiang Hospital of Southern Medical University, Guangzhou, Guangdong 510282; [4]Research Center for Tissue Engineering, Southern Medical University, Guangzhou, Guangdong 510515, P.R. China

Received October 28, 2013; Accepted April 14, 2014

DOI: 10.3892/mmr.2014.2280

Abstract. Human adipose-derived stem cells (ASCs) isolated from various body sites have been widely investigated in basic and clinical studies. However, ASCs derived from human breast tissue (hbASCs) have not been extensively investigated. In order to expand our understanding of hbASCs and examine their potential applications in stem cell research and cell-based therapy, hbASCs were isolated from discarded surgical fat tissue following reduction mammoplasty and a comprehensive characterization of these hbASCs was performed, including analysis of their cellular morphology, growth features, cell surface protein markers and multilineage differentiation capacity. These hbASCs expressed cluster of differentiation (CD)44, CD49d, CD90 and CD105, but did not express CD31 and CD34. Subsequently, the hbASCs were differentiated into adipocytes, osteocytes and chondrocytes *in vitro*. In order to examine the potential applications of hbASCs in breast reconstruction, an approach to promote *in vitro* differentiation of hbASCs into mammary gland-like epithelial cells (MGECs) was developed using activated autologous platelet-rich plasma (PRP). A proliferation phase and a subsequent morphological conversion phase were observed during this differentiation process. PRP significantly promoted the growth of hbASCs in the proliferation phase and increased the eventual conversion rate of hbASCs into MGECs. Thus, to the best of our knowledge, the present study provided the first comprehensive characterization of hbASCs and validated their multipotency. Furthermore, it was revealed that activated autologous PRP was able to enhance the differentiation efficiency of hbASCs into MGECs. The present study and other studies of hbASCs may aid the development of improved breast reconstruction strategies.

Correspondence to: Dr Hong-Mian Li, Department of Plastic and Aesthetic Surgery, Zhongshan Bo'ai Hospital of Southern Medical University, 6 Chenggui Road, Zhongshan, Guangdong 528403, P.R. China
E-mail: doctorlee2228@163.com

*Contributed equally

Key words: human breast adipose-derived stem cells, cell-based therapy, mammary gland-like epithelial cells, mammary gland regeneration, platelet-rich plasma

Introduction

Appearance restoration is an important part of treatment following cancer extirpations, including surgical excision of head and neck tumors or breast tumors, which lead to esthetic disfigurement. For instance, breast reconstruction following mastectomy is being selected by a larger number of patients (1). Given the progression of stem cell research in recent years, regenerative medicine has become a promising alternative for conventional surgical reconstruction. Restoration of stable, functional and naturally appearing tissue using different types of stem cells is an attractive method and a hot topic of investigation in the tissue engineering field. At present, numerous regenerative medicine studies focus on mesenchymal stem cells (MSCs) due to their several advantages, including easily accessible sources, differentiation plasticity, low immunogenicity and low neoplastic risk (2). It has been previously confirmed that fat tissue is a rich source of adult stem cells and these adult stem cells are termed adipose-derived stem cells (ASCs) (3). Subcutaneous adipose tissue is ubiquitous and easily accessible in large quantities through liposuction aspiration or reduction mammoplasty. As a minimally invasive procedure, liposuction surgery is a well-tolerated and safe procedure yielding large quantities of aspirate. This method is more economical and less invasive than bone marrow aspiration for stem cell isolation. Therefore, the lipoaspirate, usually discarded as medical waste, has become a popular starting material for isolating adipose-derived MSCs or stromal cells. As reported, ASCs may even be isolated from needle biopsies

of human adipose tissue or from inguinal fat pads in mice as well as from other mammals (4-8). These and other studies have provided solid evidence to support that adipose tissue contains a large number of multipotent stem cells suitable for stem cell-based therapies (9). It has been demonstrated that stem and progenitor cells in the uncultured stroma-vascular fraction of adipose tissue usually consists of up to 3% of the total cells, which is 2,500-fold higher than the ratio of stem cells in the bone marrow (4). Approximately 5,000-200,000 stem cells can be isolated from each gram of adipose tissue (10-17).

ASCs, due to their proliferation capacity, can be expanded for multiple passages without losing their multipotent properties and genomic integrity in long-term cultures (15,18,19). Numerous studies have demonstrated the plasticity of ASCs towards chondrocytes, osteoblasts, adipocytes, cardiomyocytes, smooth muscle cells and skeletal muscle cells (12,20-28). In general, *in vitro* differentiation of ASCs is achieved by culturing in selective media with lineage-specific induction factors. The possible mechanism for mesodermal lineage-specific differentiation of stem cells has been investigated in certain studies (29-34). However, the efficiency of *in vitro* differentiation of ASCs into numerous lineages, including neuronal cells and mammary gland lineages remains inadequate for clinical application and requires substantial improvements. Human ASCs have been isolated from multiple donor sites, including the abdomen and inner thigh (35-38). In addition, the isolation of ASCs from patients with gynecomastia was briefly mentioned in one study (38). Hanson *et al* previously reported isolation of ASCs from various anatomical sites, including breast (39). The data from this study suggested that the cell surface profile of ASCs does not distinguish them from normal fibroblasts, however, their differentiation capacity and pluripotency-associated gene expression clearly define ASCs as multipotent stem cells, regardless of tissue isolation location (39). Nevertheless, detailed characterization of hbASCs remains insufficient.

Platelet-rich plasma (PRP) is blood plasma with concentrated platelets. It is enriched with multiple essential growth factors (39). Several of these growth factors, including platelet-derived growth factor (PDGF), transforming growth factor β1 (TGF-β1), vascular endothelial growth factor (VEGF), fibroblast growth factor (FGF) and insulin-like growth factor-1 (IGF-1) are known to stimulate cell growth, migration, mobilization or differentiation and, therefore, have been applied in regenerative medicine. For instance, the combined use of enhanced stromal vascular fraction and PRP has been demonstrated to improve fat grafting maintenance in breast reconstruction (40,41). However, tissue regeneration is a cascade of complex, systematic events regulated by various factors. Application of a single factor usually cannot yield satisfactory therapeutic effects. In addition, the application of PRP has significant advantages over using a single growth factor and has been demonstrated to promote tissue regeneration and the wound-healing process (42). PRP has been successfully applied to treat tendon or cartilage injuries that were unable to be treated by traditional therapeutic approaches (40). Furthermore, compared with using exogenous cytokines, using autologous PRP in the clinic has fewer safety concerns as it is extracted from the same individual's venous blood. In addition to its clinical application, PRP has also been used for *in vitro* cell culture. It has been demonstrated that PRP is capable of promoting *in vitro* proliferation and differentiation of several cell types, including bone marrow-derived mesenchymal cells and ASCs (43). For instance, our previous study demonstrated that autologous PRP is capable of promoting cell proliferation and neurogenic differentiation of hASCs *in vitro* (30). These studies greatly inspired scientists to introduce PRP into the regenerative medicine field as the application of stem cells in regenerative medicine commonly requires cell expansion or differentiation *in vitro*, however, supplementation with exogenous cytokines or serums into the cell culture system has security and ethical concerns. Therefore, considering its safety and effectiveness, autologous PRP may be a powerful tool to solve these problems, thus facilitating the application of stem cells in regenerative medicine.

In the present study, in order to fill the gap in our knowledge regarding hbASCs, hbASCs were isolated from discarded surgical fat tissue from a reduction mammoplasty procedure and a series of experiments were conducted to characterize these hbASCs and examine the effect of PRP on their *in vitro* differentiation into mammary gland-like epithelial cells (MGECs).

Materials and methods

Patient consent and ethical approval. The present study was approved by the institutional ethical review board of Southern Medical University (Guangzhou, Guangdong, China). Written informed consent was provided by the donor patient.

Isolation and expansion of human breast adipose-derived stem cells (hbASCs). The hbASCs were isolated from spare fat tissue from a patient who underwent reduction mammoplasty. The fat tissue was cut into small sections and was washed with phosphate-buffered saline (PBS) to eliminate red blood cells. Then, the adipose tissue was finely minced and digested with 0.1% collagenase for 60 min at 37˚C with vigorous agitation. Following centrifugation at 260 x g for 5 min, the cell pellet, mainly consisting of hbASCs, was resuspended with Dulbecco's modified Eagle's medium (DMEM) plus 15% fetal bovine serum (FBS). The suspended cells were seeded onto dishes to expand the hbASCs. The cultures were incubated at 37˚C with 5% carbon dioxide. The first medium change was conducted 24 h after seeding and nonadherent cells were discarded. The possibility of residual mammary epithelial cells remaining in the hbASC culture was minimized through cautious procedures in the initial isolation and expansion period. Contamination of mammary epithelial cells was not observed in any hbASC cultures used for the following characterization and differentiation assays. Thereafter, the medium was replaced every 3 days. Specific differentiation medium and culture conditions are described in the following relevant results sections.

Analysis of cell surface protein markers. To identify specific cellular surface markers, hbASCs at the third passage were stained with fluorescence-conjugated cluster of differentiation (CD)31, CD34, CD44, CD49d, CD90 and CD105. The primary antibodies used were monoclonal mouse anti-human (1:200; Sigma, St. Louis, MO, USA) and the secondary antibodies

were goat anti-mouse IgG-Cy3 monoclonal antibody (CD31, CD49d and CD105) or IgG-fluorescein isothiocyanate (CD34, CD44 and CD90; all 1:100; Sigma). hbASCs stained with CD49d were counterstained with propidium iodide (PI), while hbASCs stained with CD31, CD34, CD44, CD90 and CD105 were counterstained with 4',6-diamidino-2-phenylindole, dihydrochloride (DAPI).

Staining was performed according to the following procedures: i) fixation with 4% paraformaldehyde for 30 min, followed by washing with PBS three times for 5 min; ii) treatment with 3% H_2O_2 and incubation at room temperature for 10 min, followed by washing three times with PBS for 5 min; iii) treatment with 2 mol/l hydrochloric acid and incubation for 30-45 min at room temperature, followed by washing three times with PBS for 5 min; iv) blocking with goat serum (1:20) for 20 min; v) Primary antibody incubation for 16 h at 4˚C, followed by washing three times with PBS for 5 min; vi) secondary antibody incubation for 45 min at 37˚C, followed by washing three times with PBS for 5 min; vii) counterstaining with PI or DAPI.

Preparation of PRP and measurement of growth factor concentrations. PRP was obtained from the venous blood of the same patient who underwent reduction mammoplasty. PRP was prepared via double centrifugation of the blood. In brief, 9 ml of venous blood was drawn into a polypropylene tube containing 1 ml of anticoagulant (acid citrate dextrose; Agilent Technologies, Santa Clara, CA, USA). The blood was centrifuged at 300 x g for 10 min at 25˚C to separate out the blood cell components. The upper phase containing PRP was transferred into a new tube and then centrifuged at 600 x g for an additional 10 min at 25˚C to separate out the platelet-poor plasma (PPP) in the upper phase (Fig. 1). The platelet pellets were resuspended in 1 ml of plasma and were pooled as PRP. To activate the platelets, one part of bovine thrombin stock solution (1,000 U/ml; Sigma) was added to nine parts of PRP to yield a final thrombin concentration of 100 U/ml. The mixture was incubated for 1 h at 37˚C for clot preparation. The supernatants obtained from the clot preparation were referred to as activated PRP. The PRP was stored at -80˚C until use. The concentrations of growth factors, including PDGF, TGF-β, VEGF, FGF and IGF-1, were measured using commercially available Quantikine colorimetric sandwich ELISA kits (R&D Systems, Minneapolis, MN, USA) according to the manufacturer's instructions.

Application of PRP for the differentiation of MGECs from hbASCs. The hbASCs at the third passage were seeded onto six-well culture plates. When the cell culture reached 70-80% confluency, the medium was aspirated and replenished with medium A containing PRP and medium B without PRP for the test group and the control group, respectively. Medium A contained 20 μg/ml insulin, 2 μg/ml hydrocortisone, 20 μg/ml prolactin, 20 μg/ml corporin and 10% PRP in its base medium, low glucose-DMEM. Medium B did not contain 10% PRP and the remaining ingredients were the same as those of medium A. The cellular morphology was examined every 24 h under an inverted microscope in phase-contrast and three-dimensional modes (Leica Microsystems AG, Wetzlar, Germany). The conversion rate was calculated based on the number of MGECs among every 100 random cells. In addition, hbASCs at passage 3 were also harvested and seeded onto 96-well culture plates at an equal cell density with media A and B for the proliferation assay. Cell Counting kit-8 (CCK-8) tests were performed over 7 days to establish growth curves for the two groups.

Protein extraction and western blotting. Following 4 weeks of MGEC differentiation culturing, 10 samples of each test and control group were harvested to prepare whole cell extracts (WCEs). Briefly, confluent cells were washed with ice-cold PBS and collected by scraping off the plates. Cell pellets were sonicated in extraction buffer to obtain WCEs in which the protein concentrations were subsequently quantified using the Bio-Rad DC protein assay kit (Bio-Rad, Hercules, CA, USA). Equal quantities of protein were resolved by 4-12% gradient sodium dodecyl sulfate polyacrylamide gel electrophoresis and transferred onto polyvinylidene fluoride membranes (Millipore, Bedford, MA, USA). The membranes were then incubated with blocking solutions (Pierce Biotechnology, Inc., Rockford, IL, USA) followed by primary and secondary antibody incubation. The primary antibodies used were monoclonal mouse anti-human cytokeratin (CK)-18 and monoclonal mouse anti-human CK-19 (Abcam Co. Ltd., Cambridge, UK). Goat anti-mouse monoclonal horseradish peroxidase-conjugated secondary antibodies and enhanced chemiluminescence substrate (Super-signal West Dura detection system; Pierce Biotechnology, Inc.) were used for primary antibody detection.

RNA extraction and quantitative reverse transcription polymerase chain reaction (qRT-PCR). qRT-PCR was performed to assess the expression of MGEC marker genes, including cytokeratin-19 (CK-19), *α-casein* and *β-casein*. Total RNA was isolated from monolayer cultures with the Ultraspec RNA purification kit (Biotecx Laboratories Inc., Houston, TX, USA) according to the manufacturer's instructions. Reverse transcription was performed with 2 μg of total RNA using the Superscript RT II kit (Life Technologies, Rockville, MD, USA) and random primers. qPCR was performed with the DyNamo SYBR Green qPCR kit using an MJ Research Opticon 2 real-time PCR machine according to the manufacturer's instructions (MJ Research, Reno, NV, USA). Melting curve analysis and agarose gel electrophoresis were performed to determine the purity of the PCR products. *β-actin* was used as an internal control. The comparative threshold cycle (Ct) method was used to calculate the relevant concentration of target genes (42). The PCR primers are listed in Table I.

Statistical analysis. qRT-PCR was repeated six times and the results are expressed as the mean ± standard deviation. The PCR and western blotting results were compared using the unpaired Student's t-test. $P<0.05$ was considered to indicate a statistically significant difference. All statistical analyses were performed using SPSS® version 16.0 software (SPSS, Inc., Chicago, IL, USA).

Results

Characterization of hbASCs. Following initial isolation and expansion, homogeneous hbASCs that grew in a monolayer

Table I. Primer sequences.

Gene name (human)	Forward primer sequence (5' to 3')	Reverse primer sequence (5' to 3')
CK-19	CTTCCTACAGCTATCGCCAG	TCCGTCTTGCTGATCTGCAG
α-casein	GACAACCATGAAACTTCTCATC	CTCACCACAGTGGCATAGTA
β-casein	AGGAACAGCAGCAAACAG	TTTCCAGTCGCAGTCAAT
GAPDH	GGTGAAGGTCGGAGTCAACG	CAAAGTTGTCATGGATGHACC

CK-19, cytokeratin-19.

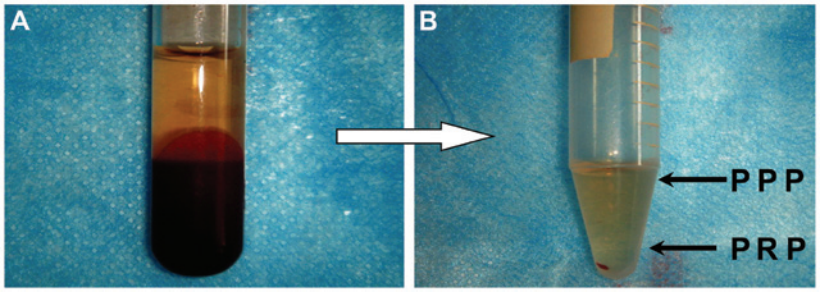

Figure 1. Isolation of PRP and PPP from venous whole blood. (A) Preparation tube following the first centrifugation. The upper phase containing platelets were transferred into a new tube for a second centrifugation. Blood cell elements were in the lower phase. (B) Preparation tube following the second centrifugation. The lower phase was collected as PRP. The small red cell pellet at the bottom was not collected into the final PRP preparation. PRP, platelet-rich plasma; PPP, platelet-poor plasm.

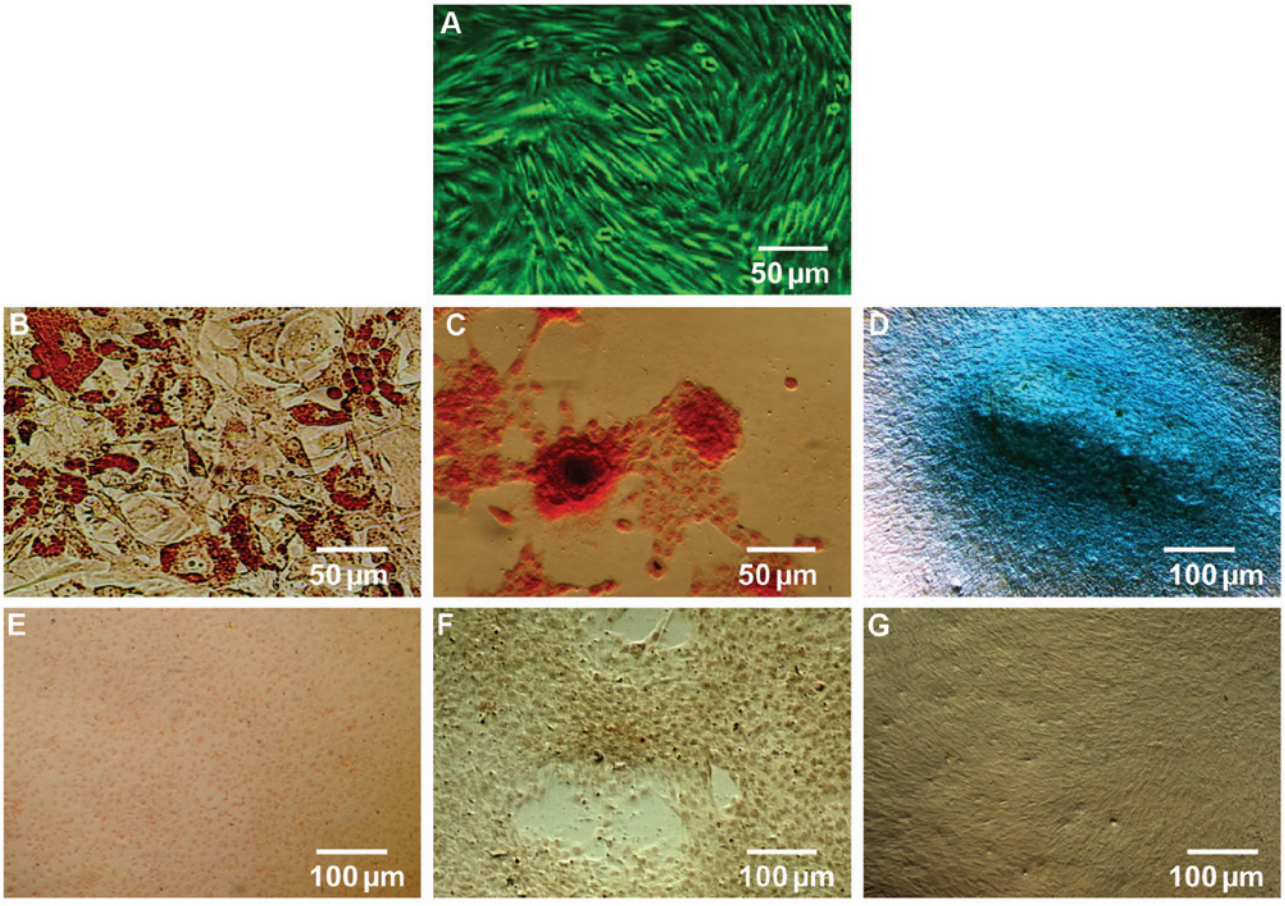

Figure 2. Characterization of hbASCs prior to and following induction culturing. (A) hbASCs at passage 3. (B) Oil red O staining of hbASCs following induction culturing for 2 weeks. (C) Alizarin red staining of hbASCs following induction culturing for 3 weeks. (D) Alcian blue staining of hbASCs following induction culturing for 2 weeks. (E, F and G) Positive staining was not observed in any of the control groups. Scale bars: 50 μm in A, B and C; 100 μm in D, E, F and G. (A-C, magnification, x200; D-G, magnification, x100). hbASCs, human breast tissue adipose-derived stem cells.

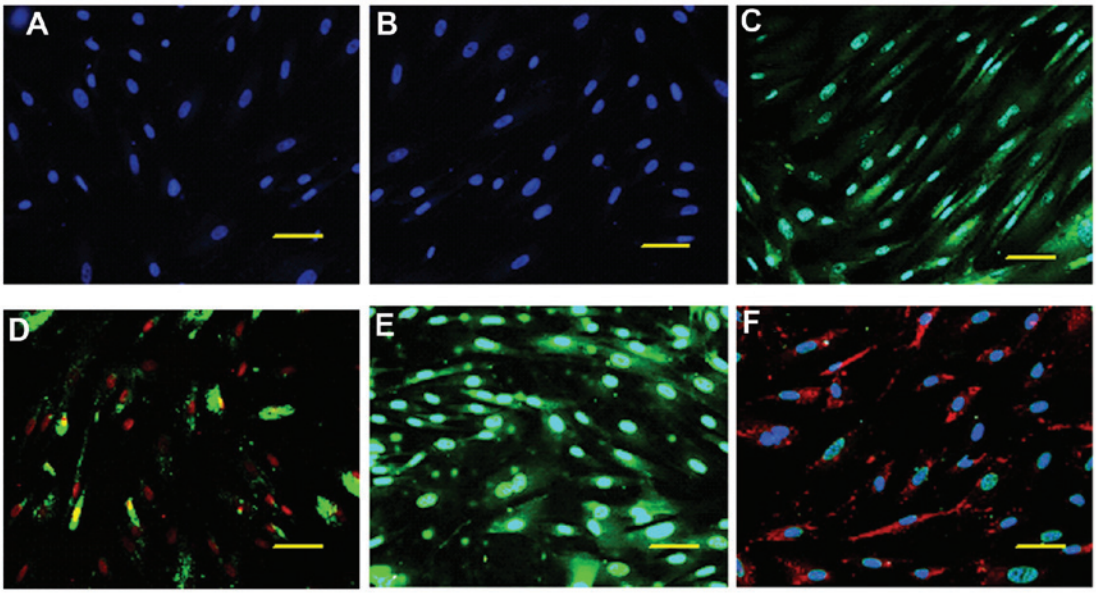

Figure 3. Characterization of human breast tissue adipose-derived stem cells at the third passage (magnification, x100). (A) Negative for CD31 staining; (B) negative for CD34 staining; (C) positive for CD44 staining; (D) positive for CD49d staining; (E) positive for CD90 staining; (F) positive for CD105 staining. The nuclei in panel D were counterstained with propidium iodide (red) and nuclei in other panels were counterstained with 4',6-diamidino-2-phenylindole, dihydrochloride (blue). Scale bars: 100 μm. CD, cluster of differentiation.

with spindle-shaped morphology were observed following culturing for ~2 weeks (Fig. 2A). These hbASCs presented a strong proliferation capacity. The hbASCs reached 80-90% confluency 7 days after initial seeding for the first passage. In subsequent culturing, these cells reached the same confluency within 3-4 days with a 1:3 split ratio. These observations demonstrated that hbASCs resemble other ASCs in terms of morphology and proliferation capacity (11,44). It has been reported that MSCs derived from different tissue sources express similar but nonidentical patterns of cell surface markers, possibly due to differences in tissue source and donor age (45,46). CD105, CD90 and CD44 are the main three positive markers for MSCs. While CD34 is the most frequently reported negative marker. CD49d and CD31 have also been reported as a positive marker and a negative marker, respectively (45). In order to define the cellular features of hbASCs, all above-mentioned cell surface markers were analyzed in the hbASCs isolated in the present study. The hbASCs at the third passage were subjected to immunofluorescence staining with antibodies against these marker proteins. The immunofluorescence staining results demonstrated that these hbASCs express CD44, CD49d, CD90 and CD105 (>90% cells are positive for staining), however, do not express CD31 or CD34 (<5% cells are positive for staining; Fig. 3).

Multipotency of hbASCs. To validate the multilineage differentiation capacity of the isolated hbASCs, subconfluent hbASCs at passage 3 were cultured for 1-3 weeks with osteogenic, adipogenic and chondrogenic induction media as listed in Table II. The lineage-specific cell morphology was observed following 1, 2 and 3 weeks of inductive culturing for adipocytes, osteocytes and chondrocytes, respectively. Positive staining of oil Red-O, alizarin red or alcian blue typically indicate adipocytes, osteocytes or chondrocytes, respectively. Thus, lineage-specific histological staining was performed with these dyes and the results confirmed that the hbASCs were differentiated into adipocytes, osteocytes and chondrocytes following relevant inductive culturing (Fig. 2B-D). Positive staining was not observed in any of the control groups (Fig. 2E-G). These results validated the multipotency of hbASCs.

Effect of PRP on hbASC proliferation and their conversion to MGECs. The PRP was prepared from the same patient's venous whole blood (VWB) by the double centrifugation approach as described in the Materials and methods section (Fig. 1). The platelet density was markedly increased in PRP compared with that in the original VWB. The mean values of the platelet density were (136.12±21.73) x 10^9/l and (892.07±41.25) x 10^9/l in VWB and PRP, respectively, revealing a 655.36% increase in PRP. Consistently, the concentrations of essential growth factors, including PDGF, TGF-β1, VEGF, FGF and IGF-1 in PRP were increased >100-fold in PRP compared with VWB (Table III).

In order to examine the effect of PRP on hbASC proliferation during MGEC differentiation, growth curves were established using the CCK-8 for hbASCs cultured in medium A containing 10% PRP and in control medium B without PRP, which were designated as the test group and the control group, respectively. A proliferation phase in the first 6 days and a subsequent morphological conversion phase were observed during the differentiation process for the test and the control groups (Fig. 4). These data further revealed that PRP significantly promoted hbASC growth in the proliferation phase. Following initial equivalent seeding, the absorbance values of the test group, which were positively associated with the cell densities, were significantly greater than those of the control group ($P<0.001$) at day 3 of differentiation (Fig. 4). The proliferation difference between the two groups continued to increase until the cells reached the growth plateau on

Table II. Multilineage induction of adipose-derived stem cells.

Lineage	Induction media	Characterization
Adipogenic	DMEM (high glucose), 10% FBS, 1% antibiotic/antimycotic, 200 μM indomethacin, 0.5 mM isobutyl-methylxanthine, 1 μM dexamethasone, 10 μM insulin,	Oil red O staining
Osteogenic	DMEM (high glucose), 10% FBS, 1% antibiotic/antimycotic, 0.1 M dexamethasone, 50 μM ascorbate-2-phosphate, 10 mM b-glycerophosphate,	Alizarin red staining
Chondrogenic	DMEM (high glucose), 1% FBS, 10 ng/ml TGF-β1, 1% antibiotic/antimycotic, 6.25 μg/ml insulin, 50 nM ascorbate-2-phosphate	Alcian blue staining

DMEM, Dulbecco's modified Eagle's medium; FBS, fetal bovine serum; TGF-β1, transforming growth factor β1.

Table III. Concentrations of growth factors in PRP and in VWB (ng/ml).

Growth factor	Concentration in PRP	Concentration in VWB
PDGF	719.25±63.04	6.65±1.27
TGF-β1	694.08±58.92	5.91±0.58
VEGF	1127.36±70.43	8.03±1.35
FGF	865.79±67.55	7.21±1.33
IGF-1	623.17±45.37	5.12±0.64

PRP, platelet-rich plasma; VWB, venous whole blood; PDGF, platelet-derived growth factor; TGF-β1, transforming growth factor β1; VEGF, vascular endothelial growth factor; FGF, fibroblast growth factor; IGF-1, insulin-like growth factor 1.

day 6, when morphology conversion started. However, it is noteworthy that the timeline for the transition between the proliferation phase and the conversion phase was the same for the two groups. On day 6 of differentiation, the cellular morphology altered from a spindle-like shape to a polygonal or circle-like shape in the two media groups, resembling the morphology of MGECs (Fig. 5) (47). Following 4 weeks of induction culturing, the polygonal or circle-like cells formed clusters and developed into colonies (Fig. 5). More colonies were observed in the test group cultured with PRP than in the control group. The conversion rate of MGECs in the test group (35.13±6.02%) was significantly increased compared with that in the control group (11.24±3.27%; P<0.01).

CK-18 and CK-19 are two cytokeratin proteins expressed in MGECs (48). Therefore, the protein expression levels of CK-18 and CK-19 in the cells following 4 weeks of induction culturing were analyzed by western blot analysis to evaluate the differentiation outcomes. The protein levels of CK-18 and CK-19 in the test group were >2-fold greater than those in the control group (P<0.001; Fig. 6). Consistently, the mRNA levels of the MGEC markers *CK-19*, *α-casein* and *β-casein* in the test group were approximately three times of those in the control group (P<0.01; Fig. 7).

Overall, the cell growth, morphology conversion and expression of marker gene results consistently demonstrated that PRP promoted the proliferation of hbASCs and subsequently increased their conversion rate to MGECs during this differentiation process.

Discussion

Given their proliferation and multilineage differentiation capacity, ASCs have become an attractive subject in regenerative medicine and have been applied in several clinical trials regarding breast reconstruction, repair of craniofacial defects, treatment of cardiovascular diseases and chronic wound healing (49). However, to the best of our knowledge, hbASCs derived from human breast adipose tissue have neither been carefully characterized nor been actively employed in studies. In the present study, hbASCs were isolated and their features were analyzed, including their cellular morphology, antigen pattern on the cell surface, proliferation capacity and multipotency. Data from the present study demonstrated that hbASCs resemble other ASCs in all these aspects.

The hbASCs in culture adhered to the dish surface and appeared as a fibroblast-like spindle shape (Fig. 2A, 5A and 5B), thus, exhibiting the typical morphology of ASCs (11,50,51). The hbASCs grew at a rate of 3 days per passage when cultured in standard medium, indicating a strong proliferation capacity. As reported, ASCs present a similar cell surface expression

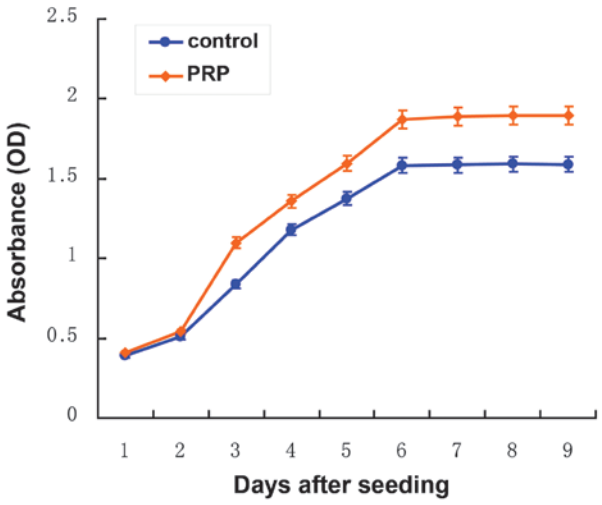

Figure 4. Cell proliferation assay using the cell counting kit-8 test. Since day 3, the PRP group (red curve) displayed a significantly greater absorbance value compared with the control group (blue curve; P<0.001). PRP, platelet-rich plasma; OD, optical density.

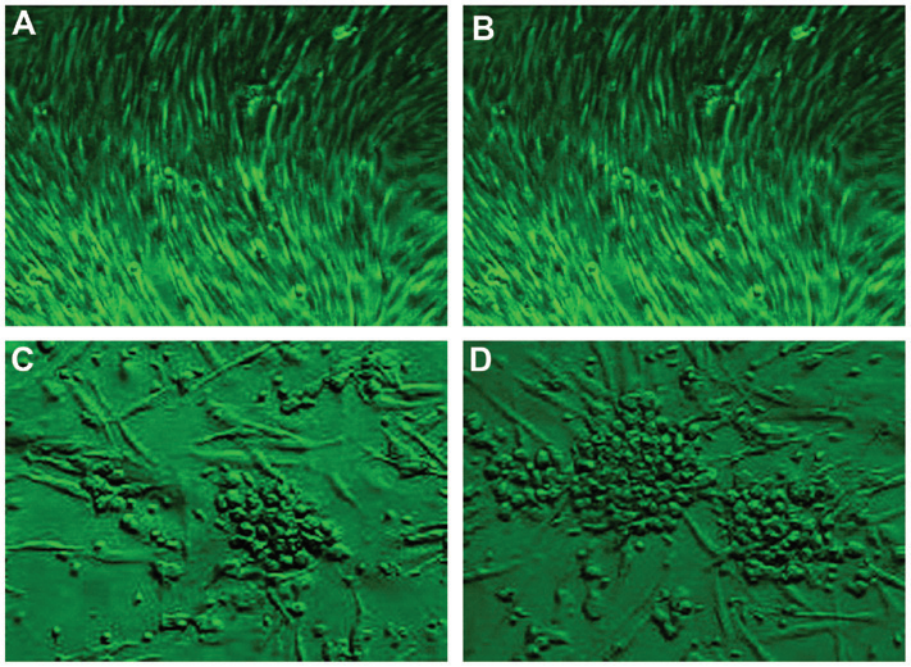

Figure 5. Alteration in cellular morphology during mammary gland-like epithelial cell differentiation. (A) hbASCs prior to induction in the control group without the addition of platelet-rich plasma. (B) hbASCs prior to induction in the test group with the addition of 10% PRP. (C) Cells in the control group following induction for 4 weeks. Cells with polygonal or circle-like morphology presented in the culture at a lower density. Fewer clusters (colonies) were observed than in the test group. (D) Cells in the test group following induction for 4 weeks. Cells with polygonal or circle-like morphology presented in the culture with a greater density. More clusters were observed in the test group compared with the control group. Scale bars: 80 μm. hbASCs, human breast tissue adipose-derived stem cells.

profile as that of bone marrow stromal cells (39). Analysis of cell surface markers revealed that hbASCs express the most frequently reported MSC markers, CD105, CD90 and CD44, and do not express CD34, a well-known hematopoietic marker. The results from the present study clearly demonstrated that hbASCs, a subtype of ASCs, are similar to the majority of MSCs in terms of cell surface markers. The absence of CD34 expression indicated a high purity of hbASCs and excluded the possibility of hematopoietic stem cell contamination in our cultures. Of note, the hbASCs were positive for CD49d but negative for CD31. The expression/absence of these markers has been observed in a few reported MSCs, depending on the tissue source (45). Thus, the unique expression pattern of these two markers plus the MSC-resembling expression pattern of the aforementioned four markers in hbASCs constitute the hbASC-specific expression pattern of cell surface markers, which is useful for defining hbASCs and developing a flow cytometric sorting approach in future hbASC studies.

hbASCs, being a subtype of MSCs, presumably possess a certain range of differentiation potency as that of MSCs. A series of proof-of-concept differentiation experiments were performed in the present study to examine the multipotency

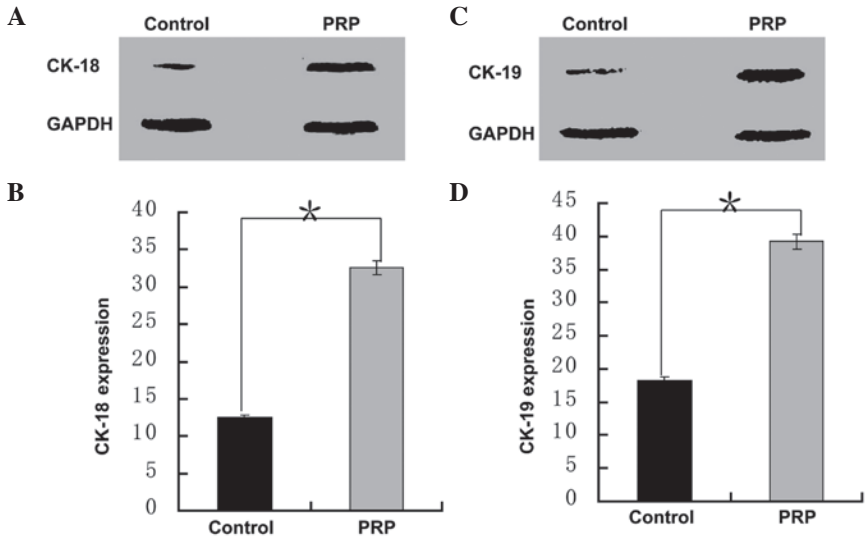

Figure 6. Effects of PRP on mammary gland-like epithelial cell differentiation of human breast tissue adipose-derived stem cells. (A) Western blot image of CK-18. (B) Quantification of western blot results for CK-18. *P<0.001, compared with the control group. (C) Western blot image of CK-19. (D) Quantification of western blot results for CK-19. *P<0.001, compared with the control group. GAPDH was used as a control. PRP, platelet-rich plasm; CK, cytokeratin.

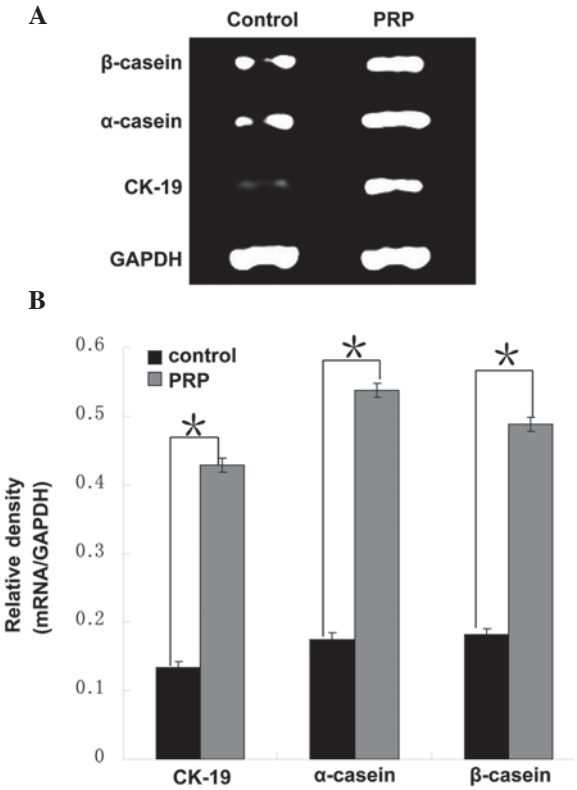

Figure 7. Effects of PRP on mammary gland-like epithelial cell differentiation of human breast tissue adipose-derived stem cells. (A) RT-PCR results for *CK-19*, *α-casein* and *β-casein* expression in the test and control groups. (B) qRT-PCR of *CK-19*, *α-casein* and *β-casein*. *P<0.001, compared with the control group. GAPDH was used as a control. PRP, platelet-rich plasma; qRT-PCR, quantitative reverse transcription polymerase chain reaction; CK, cytokeratin.

of hbASCs. Similar to other MSCs, hbASCs have the potential to differentiate into adipocytes, osteocytes and chondrocytes following appropriate induction (Fig. 2B-D; Table III). Notably, hbASCs were able to differentiate into adipocytes significantly faster than into other lineages (one week versus three weeks). This phenomenon possibly reflected the fact that certain epigenetic modifications have been established in these adult stem cells so as to attribute them a greater propensity to their designated cellular fate than into other lineages. It further indicated that hbASCs may be a better stem cell resource for breast reconstruction than other types of ASCs as hbASCs are derived from breast adipose tissue and are presumably designated to produce breast tissues. These differentiation data, although preliminary, indicated that hbASCs have a similar, if not identical, multipotency to that of MSCs and implied that hbASCs may be utilized as alternative stem cell sources for MSCs in numerous clinical aspects. To complete the multipotency characterization of hbASCs, it may be noteworthy to investigate whether hbASCs are able to differentiate toward other lineages, including myogenic, neurogenic and angiogenic lineages that are able to be induced from bone marrow-derived MSCs and several types of ASCs.

ASCs are able to differentiate into epithelial lineage cells with a limited efficiency (52,53). In order to assess whether hbASCs have the same capacity, the differentiation of hbASCs into MGECs was conducted. Two phases were observed during this differentiation process: a proliferation phase between day 0 and day 6 with fast cell growth; and a subsequent conversion phase with an alteration in cellular morphology and negligible cell growth (Fig. 4). Furthermore, the effect of activated PRP from the same patient on the conversion of hbASCs to MGECs was examined in the present study. More than 100-fold enrichment of the critical growth factors was detected in the PRP preparation, indicating its good quality. PRP did not interfere with the timeline of the two phases during differentiation. However, PRP significantly promoted the growth rate and augmented cell expansion in the proliferation phase. Eventually, the greater conversion rate of MGECs, based on the alteration in cellular morphology, was observed in the differentiation culture supplemented with 10% PRP compared with that in the control group (35 vs. 11%; Fig. 5). The enhanced conversion rate stimulated by PRP was further confirmed by analyzing the expression levels of the mammary

gland epithelial markers CK-18, CK-19, α-casein and β-casein (Figs. 6 and 7). These results consistently demonstrated that activated autologous PRP is capable of promoting MGEC differentiation from hbASCs. The fact that the timeline for the transition from the proliferation phase to the conversion phase was not affected by PRP indicated that inherent cellular events are required for cell fate conversion, which PRP cannot interfere with, at least not in the proliferation phase. It is not clear whether the eventual greater conversion rate in the test group with PRP was caused by stimulation of PRP in the conversion phase or whether this greater conversion rate was simply an outcome secondary to the increased cell density caused by PRP in the proliferation phase. This question may be answered in a future study by increasing the initial hbASC density without using PRP and determining whether a similarly enhanced conversion rate (not an absolute number) is able to be achieved as with PRP addition. Overall, the data from the present study demonstrated that hbASCs are able to differentiate into MGECs and that activated autologous PRP was able to significantly increase the differentiation efficiency. These results may aid the development of approaches to utilize hbASCs in mammary gland regeneration.

In conclusion, to the best of our knowledge, the present study was the first to provide comprehensive characterization of hbASCs and demonstrated that hbASCs, being a new member of the ASC family, are generally similar to other types of ASCs in terms of cellular morphology, cell surface antigen pattern, proliferation capacity and multilineage differentiation potency. It was also revealed that activated autologous PRP is able to significantly improve the differentiation of hbASCs into MGECs, providing an efficient approach for hbASC differentiation. Overall, the information from the present study filled the gap in our knowledge regarding hbASCs and provided a fundamental basis for the application of hbASCs in future studies.

Acknowledgements

This work was financially supported by the China Postdoctoral Science Foundation (No. 20090450910) and the Medical Scientific Research Foundation of Guangdong Province, China (No. A2012814). The authors thank the Research Center of Tissue Engineering, Southern Medical University for their support, and special thanks are owed to Professor Shan Jiang.

References

1. Cordeiro PG: Breast reconstruction after surgery for breast cancer. N Engl J Med 359: 1590-1601, 2008.
2. Ren G, Chen X, Dong F, *et al*: Concise review: mesenchymal stem cells and translational medicine: emerging issues. Stem Cells Transl Med 1: 51-58, 2012.
3. Dubois SG, Floyd EZ, Zvonic S, Kilroy G, Wu X, Carling S, Halvorsen YD, Ravussin E and Gimble JM: Isolation of human adipose-derived stem cells from biopsies and liposuction specimens. Methods Mol Biol 449: 69-79, 2008.
4. Neupane M, Chang CC, Kiupel M and Yuzbasiyan-Gurkan V: Isolation and characterization of canine adipose-derived mesenchymal stem cells. Tissue Eng Part A 14: 1007-1015, 2008.
5. Peptan IA, Hong L and Mao JJ: Comparison of osteogenic potentials of visceral and subcutaneous adipose-derived cells of rabbits. Plast Reconstr Surg 117: 1462-1470, 2006.
6. Tholpady SS, Katz AJ and Ogle RC: Mesenchymal stem cells from rat visceral fat exhibit multipotential differentiation in vitro. Anat Rec A Discov Mol Cell Evol Biol 272: 398-402, 2003.
7. Vidal MA, Kilroy GE, Lopez MJ, Johnson JR, Moore RM and Gimble JM: Characterization of equine adipose tissue-derived stromal cells: adipogenic and osteogenic capacity and comparison with bone marrow-derived mesenchymal stromal cells. Vet Surg 36: 613-622, 2007.
8. Safford KM, Hicok KC, Safford SD, *et al*: Neurogenic differentiation of murine and human adipose-derived stromal cells. Biochem Biophys Res Commun 294: 371-379, 2002.
9. Jurgens WJ, Oedayrajsingh-Varma MJ, Helder MN, Zandiehdoulabi B, Schouten TE, Kuik DJ, Ritt MJ and van Milligen FJ: Effect of tissue-harvesting site on yield of stem cells derived from adipose tissue: implications for cell-based therapies. Cell Tissue Res 332: 415-426, 2008.
10. Grimes BR, Steiner CM, Merfeld-Clauss S, *et al*: Interphase FISH demonstrates that human adipose stromal cells maintain a high level of genomic stability in long-term culture. Stem Cells Dev 18: 717-724, 2009.
11. Zuk PA, Zhu M, Ashjian P, *et al*: Human adipose tissue is a source of multipotent stem cells. Mol Biol Cell 13: 4279-4295, 2002.
12. Gimble JM and Guilak F: Differentiation potential of adipose derived adult stem (ADAS) cells. Curr Top Dev Biol 58: 137-160, 2003.
13. Gimble J and Guilak F: Adipose-derived adult stem cells: isolation, characterization, and differentiation potential. Cytotherapy 5: 362-369, 2003.
14. Strem BM, Hicok KC, Zhu M, *et al*: Multipotential differentiation of adipose tissue-derived stem cells. Keio J Med 54: 132-141, 2005.
15. Fraser JK, Schreiber R, Strem B, *et al*: Plasticity of human adipose stem cells toward endothelial cells and cardiomyocytes. Nat Clin Pract Cardiovasc Med 3 (Suppl 1): S33-S37, 2006.
16. Jack GS, Almeida FG, Zhang R, Alfonso ZC, Zuk PA and Rodríguez LV: Processed lipoaspirate cells for tissue engineering of the lower urinary tract: implications for the treatment of stress urinary incontinence and bladder reconstruction. J Urol 174: 2041-2045, 2005.
17. Rodríguez LV, Alfonso Z, Zhang R, Leung J, Wu B and Ignarro LJ: Clonogenic multipotent stem cells in human adipose tissue differentiate into functional smooth muscle cells. Proc Natl Acad Sci USA 103: 12167-12172, 2006.
18. Mizuno H, Zuk PA, Zhu M, Lorenz HP, Benhaim P and Hedrick MH: Myogenic differentiation by human processed lipoaspirate cells. Plast Reconstr Surg 109: 199-209, 2002.
19. Zaman WS, Makpol S, Sathapan S and Chua KH: Long-term in vitro expansion of human adipose-derived stem cells showed low risk of tumourigenicity. J Tissue Eng Regen Med 8: 67-76, 2014.
20. Lee JH and Kemp DM: Human adipose-derived stem cells display myogenic potential and perturbed function in hypoxic conditions. Biochem Biophys Res Commun 341: 882-888, 2006.
21. Liu TM, Martina M, Hutmacher DW, Hui JH, Lee EH and Lim B: Identification of common pathways mediating differentiation of bone marrow- and adipose tissue-derived human mesenchymal stem cells into three mesenchymal lineages. Stem Cells 25: 750-760, 2007.
22. Li HX, Luo X, Liu RX, Yang YJ and Yang GS: Roles of Wnt/beta-catenin signaling in adipogenic differentiation potential of adipose-derived mesenchymal stem cells. Mol Cell Endocrinol 291: 116-124, 2008.
23. Karbiener M, Fischer C, Nowitsch S, *et al*: microRNA miR-27b impairs human adipocyte differentiation and targets PPARgamma. Biochem Biophys Res Commun 390: 247-251, 2009.
24. James AW, Leucht P, Levi B, *et al*: Sonic Hedgehog influences the balance of osteogenesis and adipogenesis in mouse adipose-derived stromal cells. Tissue Eng Part A 16: 2605-2616, 2010.
25. Davis LA and Zur Nieden NI: Mesodermal fate decisions of a stem cell: the Wnt switch. Cell Mol Life Sci 65: 2658-2674, 2008.
26. Schäffler A and Buchler C: Concise review: adipose tissue-derived stromal cells - basic and clinical implications for novel cell-based therapies. Stem Cells 25: 818-827, 2007.
27. Cousin B, André M M, Arnaud E, Pénicaud L and Casteilla L: Reconstitution of lethally irradiated mice by cells isolated from adipose tissue. Biochem Biophys Res Commun 301: 1016-1022, 2003.
28. Miranville A, Heeschen C, Sengenès C, Curat CA, Busse R and Bouloumié A: Improvement of postnatal neovascularization by human adipose tissue-derived stem cells. Circulation 110: 349-355, 2004.

29. Corre J, Barreau C, Cousin B, *et al*: Human subcutaneous adipose cells support complete differentiation but not self-renewal of hematopoietic progenitors. J Cell Physiol 208: 282-288, 2006.
30. Li H, Han Z, Liu D, Zhao P, Liang S and Xu K: Autologous platelet-rich plasma promotes neurogenic differentiation of human adipose-derived stem cells in vitro. Int J Neurosci 123: 184-190, 2013.
31. Wu J, Pan Z, Cheng M, *et al*: Ginsenoside Rg1 facilitates neural differentiation of mouse embryonic stem cells via GR-dependent signaling pathway. Neurochem Int 62: 92-102, 2013.
32. Shi AW, Gu N, Liu XM, Wang X and Peng YZ: Ginsenoside Rg1 enhances endothelial progenitor cell angiogenic potency and prevents senescence in vitro. J Int Med Res 39: 1306-1318, 2011.
33. Wang L and Kisaalita WS: Administration of BDNF/ginsenosides combination enhanced synaptic development in human neural stem cells. J Neurosci Methods 194: 274-282, 2011.
34. Shi AW, Wang XB, Lu FX, Zhu MM, Kong XQ and Cao KJ: Ginsenoside Rg1 promotes endothelial progenitor cell migration and proliferation. Acta Pharmacol Sin 30: 299-306, 2009.
35. Moshtagh PR, Emami SH and Sharifi AM: Differentiation of human adipose-derived mesenchymal stem cell into insulin-producing cells: an in vitro study. J Physiol Biochem 69: 451-458, 2013.
36. Scuderi N, Ceccarelli S, Onesti MG, *et al*: Human adipose-derived stromal cells for cell-based therapies in the treatment of systemic sclerosis. Cell Transplant 22: 779-795, 2013.
37. Kisiel AH, McDuffee LA, Masaoud E, Bailey TR, Esparza Gonzalez BP and Nino-Fong R: Isolation, characterization, and in vitro proliferation of canine mesenchymal stem cells derived from bone marrow, adipose tissue, muscle, and periosteum. Am J Vet Res 73: 1305-1317, 2012.
38. Heneidi S, Simerman AA, Keller E, Singh P, Li X, Dumesic DA and Chazenbalk G: Awakened by cellular stress: isolation and characterization of a novel population of pluripotent stem cells derived from human adipose tissue. PLoS One 8: e64752, 2013.
39. Hanson SE, Kim J and Hematti P: Comparative analysis of adipose-derived mesenchymal stem cells isolated from abdominal and breast tissue. Aesthet Surg J 33: 888-898, 2013.
40. Livak KJ and Schmittgen TD: Analysis of relative gene expression data using real-time quantitative PCR and the 2(-Delta Delta C(T)) Method. Methods 25: 402-408, 2001.
41. Smith SE and Roukis TS: Bone and wound healing augmentation with platelet-rich plasma. Clin Podiatr Med Surg 26: 559-588, 2009.
42. Gentile P, Orlandi A, Scioli MG, Di Pasquali C, Bocchini I and Cervelli V: Concise review: adipose-derived stromal vascular fraction cells and platelet-rich plasma: basic and clinical implications for tissue engineering therapies in regenerative surgery. Stem Cells Transl Med 1: 230-236, 2012.
43. Mardani M, Kabiri A, Esfandiari E, Esmaeili A, Pourazar A, Ansar M and Hashemibeni B: The effect of platelet rich plasma on chondrogenic differentiation of human adipose derived stem cells in transwell culture. Iran J Basic Med Sci 16: 1163-1169, 2013.
44. Gaiba S, França LP, França JP and Ferreira LM: Characterization of human adipose-derived stem cells. Acta Cir Bras 27: 471-476, 2012.
45. Mafi P, Hindocha S, Mafi R, Griffin M and Khan WS: Adult mesenchymal stem cells and cell surface characterization - a systematic review of the literature. Open Orthop J 5: 253-260, 2011.
46. Hass R, Kasper C, Böhm S and Jacobs R: Different populations and sources of human mesenchymal stem cells (MSC): A comparison of adult and neonatal tissue-derived MSC. Cell Commun Signal 9: 12, 2011.
47. Dimri G, Band H and Band V: Mammary epithelial cell transformation: insights from cell culture and mouse models. Breast Cancer Res: 7: 171-179, 2005.
48. Péchoux C, Gudjonsson T, Ronnov-Jessen L, Bissell MJ and Petersen OW: Human mammary luminal epithelial cells contain progenitors to myoepithelial cells. Dev Biol 206: 88-99, 1999.
49. Tobita M, Orbay H and Mizuno H: Adipose-derived stem cells: current findings and future perspectives. Discov Med 11: 160-170, 2011.
50. Zuk PA, Zhu M, Mizuno H, *et al*: Multilineage cells from human adipose tissue: implications for cell-based therapies. Tissue Eng 7: 211-228, 2001.
51. Halvorsen YD, Franklin D, Bond AL, *et al*: Extracellular matrix mineralization and osteoblast gene expression by human adipose tissue-derived stromal cells. Tissue Eng 7: 729-741, 2001.
52. Baer PC, Döring C, Hansmann ML, Schubert R and Geiger H: New insights into epithelial differentiation of human adipose-derived stem cells. J Tissue Eng Regen Med 7: 271-278, 2011.
53. Baer PC, Brzoska M and Geiger H: Epithelial differentiation of human adipose-derived stem cells. Methods Mol Biol 702: 289-298, 2011.